

How to reach a few percent level in determining the Lense-Thirring effect?

Lorenzo Iorio

Dipartimento Interateneo di Fisica dell' Università di Bari

Via Amendola 173, 70126

Bari, Italy

Eelco Doornbos

Faculty of Aerospace Engineering, Delft University Of Technology,

Kluyverweg 1, 2629 HS,

Delft, The Netherlands

Abstract

In this paper we explore the possibility of suitably combining the nodes Ω of the existing geodetic LAGEOS, LAGEOS II and Ajisai laser-ranged satellites and of the radar altimeter Jason-1 satellite in order to increase the accuracy in testing the general relativistic gravitomagnetic Lense-Thirring secular effect in the gravitational field of the Earth. The proposal of introducing Ajisai and Jason-1 in such a combination comes from the expected benefits which could be obtained in reducing the aliasing secular impact of the classical part of the terrestrial gravitational field. According to the recently released EIGEN-CG01C combined GRACE+CHAMP+terrestrial gravimetry/altimetry Earth gravity model, the impact of the static part of the mismodelled even zonal harmonics of geopotential, which represent the major source of systematic error, amounts to 1.6%, at $1-\sigma$ level. It is better than the error which could be obtained with a two-node LAGEOS-LAGEOS II only combination (6% at $1-\sigma$). Moreover, the proposed combination would be insensitive also to the secular variations of the low-degree even zonal harmonics, contrary to the LAGEOS-LAGEOS II only combination. Such variations could be a serious limiting factor over observational time spans many years long. The price to be paid for this improvements of the systematic error of gravitational origin is represented by the non-conservative forces introduced along with the new orbital elements. However, they would induce periodic perturbations, contrary to the gravitational noise. A major concern would be the assessment of the impact of the non-conservative accelerations on the Jason-1 node. According to the present-day force models, the mismodelling in the non-conservative forces would, at worst, induce an aliasing periodic signal with an amplitude of 4% of the Lense-Thirring effect over a time span of 2 years. However, an observational time

span of just some years could safely be adopted in order to fit and remove the residual long-period non-gravitational signals affecting Jason's node, which, in the case of the direct solar radiation pressure, have a main periodicity of approximately 120 days. Of course, the possibility of getting time series of the Jason's node some years long should be demonstrated in reality.

1 Introduction

1.1 The performed attempts to measure the Lense–Thirring effect with the LAGEOS satellites

The general relativistic gravitomagnetic force [1], related to the component of the gravitational field induced by the rotation of a central body of mass M and proper angular momentum J , is still awaiting for a direct, unquestionable measurement. Up to now there exist some indirect evidences of its existence as predicted by the General Theory of Relativity (GTR in the following) in an astrophysical, strong-field context [2] and, in the weak-field and slow-motion approximation valid throughout the Solar System, in the fitting of the ranging data to the orbit of Moon with the Lunar Laser Ranging (LLR) technique [3].

The direct measurement of the gravitomagnetic Schiff precession of the spins of four spaceborne gyroscopes [4] in the gravitational field of Earth is the goal of the Stanford GP-B mission [5] which has been launched in April 2004. The claimed obtainable accuracy is of the order of 1% or better.

Another consequence of the gravitomagnetic field is the Lense–Thirring effect on the geodesic path of a test particle freely orbiting a central rotating body [6]. It consists of tiny secular precessions of the longitude of the ascending node Ω and the argument of pericentre ω of the orbit of the test particle

$$\dot{\Omega}_{\text{LT}} = \frac{2GJ}{c^2 a^3 (1 - e^2)^{\frac{3}{2}}}, \quad \dot{\omega}_{\text{LT}} = -\frac{6GJ \cos i}{c^2 a^3 (1 - e^2)^{\frac{3}{2}}}, \quad (1)$$

where a , e and i are the semimajor axis, the eccentricity and the inclination, respectively, of the orbit, c is the speed of light and G is the Newtonian gravitational constant. See Figure 1.1 for the orbital geometry. The LAGEOS III/LARES mission [7, 8] was specifically designed in order to measure such effect, but, up to now, in spite of its scientific validity and relatively low cost, it has not yet been approved by any space agency or scientific institution. Recently, a drag-free version of this project [9], in the context of

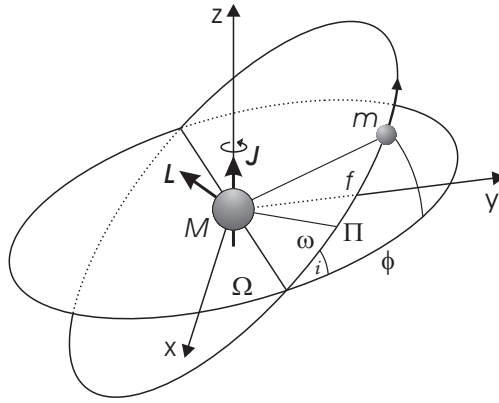


Figure 1: Orbital geometry for a motion around a central mass. Here L denotes the orbital angular momentum of the particle of mass m , J is the proper angular momentum of the central mass M , Π denotes the pericentre position, f is the true anomaly of m , which is counted from Π , Ω , ω and i are the longitude of the ascending node, the argument of pericentre and the inclination of the orbit with respect to the inertial frame $\{x, y, z\}$ and the azimuthal angle ϕ is the right ascension counted from the x axis. When orbits with small inclinations are considered, the longitude of pericentre $\varpi = \Omega + \omega$ is used.

the relativistic OPTIS mission [10], is currently under examination by the German Space Agency (DLR).

2 The current LAGEOS-LAGEOS II Lense-Thirring experiment

The Ciufolini's team analyzed the laser-ranged data to the existing geodetic LAGEOS and LAGEOS II satellites over time spans of some years [11, 12] by using the following $J_2 - J_4$ -free¹ linear combination of the orbital residuals of the nodes of LAGEOS and LAGEOS II and the perigee of LAGEOS II [13]

$$\delta\dot{\Omega}^{\text{LAGEOS}} + c_1\delta\dot{\Omega}^{\text{LAGEOS II}} + c_2\delta\dot{\omega}^{\text{LAGEOS II}} \sim \mu_{\text{LT}}60.2, \quad (2)$$

where $c_1 = 0.304$, $c_2 = -0.350$ and μ_{LT} is the solved-for least squares parameter which is 0 in Newtonian mechanics and 1 in the GTR². The residuals of the nodal and perigee rates $\delta\dot{\Omega}$ and $\delta\dot{\omega}$ are determined by comparing these orbital elements at the end of two orbit computation arcs covering the same time span. These orbit computations consist of a precise orbit, which has been adjusted to fit the available tracking data, and a predicted orbit, starting from an initial state vector which it shares with the precise orbit, but for which the later states are based on integration of the classical force models, without adjustment to the tracking data. The residuals of the rate of change of the orbital elements are then calculated by dividing the difference between these two elements by the time span of the arc. The signature of the gravitomagnetic force, assumed as an unmodelled effect, is a linear trend in the combination of the accumulated residuals, with a slope of 60.2 milliarcseconds per year (mas yr^{-1} in the following).

The latest, 2002, measurement of the Lense-Thirring effect with (2), obtained by processing the LAGEOS and LAGEOS II data over a time span of almost 8 years with the orbital processor GEODYN II of the Goddard Space Flight Center, yields [12]

$$\mu_{\text{LT}} \sim 1 \pm 0.02 \pm \delta\mu_{\text{LT}}^{\text{systematic}}, \quad (3)$$

¹ J_2 and J_4 are the first two even zonal harmonic coefficients of the multipolar expansion of the terrestrial gravitational field. It turns out that they induce secular precessions on Ω and ω . Their mismodelled parts, according to the currently available Earth gravity models, are of the same order, or even larger, than the gravitomagnetic secular precessions of interest.

²It can be expressed in terms of the PPN parameter γ as $\mu_{\text{LT}} = \frac{1+\gamma}{2}$. For the PPN formalism see [14, 1, 15].

where $\delta\mu_{\text{LT}}^{\text{systematic}}$ accounts for all the possible systematic errors due to the mismodelling in the various competing classical forces of gravitational and non-gravitational origin affecting the motion of the LAGEOS satellites. In [12] $\delta\mu_{\text{LT}}^{\text{systematic}}$ is estimated to be of the order of

$$\delta\mu_{\text{LT}}^{\text{systematic}} = 20 - 30\%. \quad (4)$$

2.1 Some possible criticisms to the performed attempts to measure the Lense–Thirring effect with the LAGEOS satellites

However, it must be pointed out that several remarks have been made by other scientists about the estimate (4) [16, 17]. First of all, it is based on assuming a 13% systematic error due to the mismodelling in the even zonal harmonics of geopotential. This result has been obtained from the full covariance matrix of the EGM96 Earth gravity model [18] up to degree $\ell = 20^3$. In the EGM96 solution the recovered even zonal harmonics are strongly reciprocally correlated; it seems, e.g., that this value for the systematic error due to geopotential is due to a lucky correlation between J_6 and J_8 which are not cancelled by (2). The point is that, according to [16, 17], nothing would assure that the covariance matrix of EGM96, which is based on a multi-year average that spans the 1970, 1980 and early 1990 decades, would reflect the true correlations between the even zonal harmonics during the particular time intervals of a few years adopted in the analyses by Ciufolini and coworkers. Then, a more conservative, although pessimistic, approach would be to consider the sum of the absolute values of the errors due to the single even zonal as representative of the systematic error induced by our uncertainty in the terrestrial gravitational field according to EGM96 [19, 20]. In this case we would get a pessimistic upper bound of 83%.

Also the use of the perigee of LAGEOS II in (2) sheds shadows on the estimate of (4). Indeed, it turns out that the perigee of the LAGEOS-like satellites is very sensitive to a whole host of non-gravitational perturbations of radiative [21] and thermal origin [22], whose impact on the proposed measurement of the Lense–Thirring effect would be very difficult to reliably assess [16, 17]. It should also be pointed out that at the time of the analyses by Ciufolini and coworkers, non-gravitational perturbations of thermal origin, such as the solar Yarkovsky–Schach effect, were not present at all in

³In fact, it turns out that the result does not change if the even zonal harmonics of degree higher than $\ell = 12$ are neglected in the calculation.

the force models of the orbital determination software GEODYN II, which was used in their analyses.

3 The new perspectives opened up by the CHAMP and GRACE models

The recent and forthcoming improvement in our knowledge of the Earth gravity field thanks to CHAMP [23] and especially GRACE [16], opens new possibilities to obtain a more accurate and reliable measurement of the Lense–Thirring effect with the LAGEOS satellites as well as the other currently existing laser–tracked satellites. In the pre–CHAMP and GRACE era these other satellites would have been unsuitable [24] because of their sensitivity to the higher degree even zonal harmonics of geopotential, due to their smaller altitude with respect to LAGEOS and LAGEOS II. In [20] a new observable has been explicitly put forth, which consists of a J_2 –free combination of the nodes of LAGEOS and LAGEOS II only. It is⁴

$$\delta\dot{\Omega}^{\text{LAGEOS}} + q_1\delta\dot{\Omega}^{\text{LAGEOS II}} \sim \mu_{\text{LT}}47.9, \quad (5)$$

with $q_1 = 0.546$. According to the recently released EIGEN-CG01C Earth gravity model⁵ [25], the systematic error due to the remaining uncanceled even zonal harmonics J_4 , J_6 , J_8 ... amounts to 5%. This result has been obtained with a 1- σ RSS (Root Sum Square) calculation based on the variance matrix of EIGEN-CG01C because, contrary to EGM96 and the other previous Earth gravity models, in this case the recovered multipolar coefficients are well disentangled. A pessimistic 1- σ upper bound of 6% can be obtained by summing the absolute values of the individual errors.

Note also that the combination (5) preserves one of the most important features of the combination (2) of orbital residuals: indeed, it allows to cancel out the very insidious 18.6-year tidal perturbation which is a $\ell = 2$, $m = 0$

⁴The possibility of using only the nodes of the LAGEOS satellites in view of the more accurate GRACE Earth gravity solutions was presented for the first time in [16], although without quantitative details.

⁵Such model represents a long-term averaged solution which combines data from CHAMP (860 days), GRACE (109 days) and surface gravimetry/altimetry; moreover, the released sigmas of the spherical harmonic coefficients of the geopotential are not the mere formal statistical errors, but are calibrated, although preliminarily. Then, guesses of the impact of the systematic error due to the geopotential on the measurement of the Lense–Thirring effect based on this solution should be rather realistic. However, caution is advised in considering the so obtained evaluations because of the uncertainties of the calibration process which affect especially the even zonal coefficients [17].

constituent with a period of 18.6 years due to the Moon’s node and nominal amplitudes of the order of 10^3 mas on the nodes of LAGEOS and LAGEOS II [26]. On the other hand, the impact of the non-gravitational perturbations on the combination (5) over a time span of, say, 7 years could be quantified in 0.1 mas yr^{-1} , yielding a 0.3% percent error. The results of Table 2 and Table 3 in [8] have been used. It is also important to notice that, thanks to the fact that the periods of many gravitational and non-gravitational time-dependent perturbations acting on the nodes of the LAGEOS satellites are rather short, a reanalysis of the LAGEOS and LAGEOS II data over not too many years could be performed. As already pointed out, this is not so for the combination (2) because some of the gravitational [26] and non-gravitational [21] perturbations affecting the perigee of LAGEOS II have periods of many years.

A possible weak point of (5) could be represented by the fact that it is affected by the secular variations of the uncanceled even zonal harmonics $\dot{J}_4, \dot{J}_6, \dots$. For the topic of \dot{J}_ℓ , which has recently received great attention by the geodesists’ community in view of unexpected variations of⁶ J_2 , see [27]. The mismodelled shift of (5) due to the secular variations of the uncanceled even zonal harmonics can be written as

$$\sum_{\ell=2} \left(\dot{\Omega}_{\ell}^{\text{LAGEOS}} + q_1 \dot{\Omega}_{\ell}^{\text{LAGEOS II}} \right) \frac{\delta \dot{J}_\ell}{2} T_{\text{obs}}^2, \quad (6)$$

where the coefficients $\dot{\Omega}_{\ell}$ are $\partial \dot{\Omega}_{\text{class}} / \partial J_\ell$ and have been explicitly calculated up to degree $\ell = 20$ in [19]. It must be divided by the gravitomagnetic shift of (5) over the same observational time span

$$\left(\dot{\Omega}_{\text{LT}}^{\text{LAGEOS}} + q_1 \dot{\Omega}_{\text{LT}}^{\text{LAGEOS II}} \right) T_{\text{obs}} = 47.9 \text{ mas yr}^{-1} T_{\text{obs}}. \quad (7)$$

By assuming $\delta \dot{J}_4 = 0.6 \times 10^{-11} \text{ yr}^{-1}$ and $\delta \dot{J}_6 = 0.5 \times 10^{-11} \text{ yr}^{-1}$ (Cox *et al* 2002), it turns out that the $1\text{-}\sigma$ percent error on the combination (5), which grows linearly with T_{obs} , would amount to 1% over one year. However, it must be pointed out that it is very difficult to have reliable evaluations of the secular variations of the higher degree even zonal harmonics of geopotential also because very long time series from the various existing laser-ranged targets are required.

Recently, (5) has been adopted for a 11-years analysis [28] based on the 2nd generation GRACE-only EIGEN-GRACE02S Earth gravity model [29],

⁶Fortunately, any issues concerning \dot{J}_2 do not affect the combination (5).

although the claimed total accuracy of the performed test might be rather optimistic [30].

Since GRACE is expected to improve especially the mid to high degree part of the spectrum of the even zonals, in [20] a $J_2 - \dots J_8$ -free combination involving the nodes of the spherical geodetic satellites LAGEOS, LAGEOS II, Ajisai, Starlette and Stella⁷ is proposed. This combination would be affected just by the higher degree J_ℓ and would be insensitive to the secular variations of the lower degree even zonal harmonics. However, due to the low altitude of Starlette and Stella, the $1\text{-}\sigma$ error due to the static part of the geopotential would still amount to 10% (RSS calculation) with a $1\text{-}\sigma$ upper bound of 31%, according to the present-day EIGEN-CG01C model. It may be interesting to note that the combination (2) would be affected less than 1% by the mismodelling in the static part of geopotential.

4 The use of the laser-ranged satellite Ajisai and of the radar altimeter satellite Jason-1

Up to now, the attention has been focused exclusively on the spherical laser-ranged satellites because of the high accuracy with which it is possible to determine their orbits. It is so also thanks to their high altitude, small area-to-mass S/M ratio and spherical shape, which reduces the impact of the non-gravitational perturbations. A recent, important achievement in orbit determination regards Jason-1. It is a radar altimeter satellite, launched on December 7, 2001, as a follow-on to the very successful TOPEX/Poseidon mission which was launched in 1992. The satellite carries state-of-the-art hardware for the three most accurate tracking systems available: Satellite Laser Ranging (SLR), Doppler Orbitography and Radiopositioning Integrated by Satellite (DORIS) and Global Positioning System (GPS). In addition, its radar altimeter measurements over the oceans can be used for either independent orbit validation, or as additional tracking data. In [31] it has been shown that it is possible to reach the 1-cm level in determining its orbit (in the radial direction) by using this dense coverage of precise tracking data.

This is a very important result, because the orbital parameters of Jason-1⁸ make it suitable to be used, in principle, for the purpose of an accurate and

⁷The current RMS of fit of the computed orbits to the laser data of these satellites is of the order of 1 cm or even better, especially for the LAGEOS satellites.

⁸One could argue that TOPEX/Poseidon, with the same orbital parameters as Jason-1, a smaller area-to-mass ratio and a 12-year (and counting) lifetime, would be the more

reliable measurement of the Lense–Thirring effect, provided that accurate force models are available for a dynamic orbit determination. Indeed, the Jason–1 orbit parameters are rather similar to those of the geodetic Ajisai satellite. In Table 1 the orbital parameters of the LAGEOS satellites and of Ajisai and Jason–1 are reported. However, it must be preliminarily pointed out that special care should be taken in handling the orbital manoeuvre burns of Jason–1, which are designed to counteract the drifting of the orbit and keep it on its repeating ground–track, as well as the infrequent safe–mode periods, which also complicate the dynamic modelling. These events do not prevent us from measuring any long–term drifts in the node however, as long as the orbital arcs are designed to start after and stop just before these instances. Because the manoeuvres are mostly performed in pairs, approximately one hour apart, and the two safe–mode periods up to now have lasted several days, they would however introduce uncertainties when fitting for long–period signals.

Table 1: Orbital parameters, predicted Lense–Thirring nodal rates $\dot{\Omega}_{\text{LT}}$ and approximate area–to–mass ratios S/M . a, e, i and n are the semimajor axis, the eccentricity, the inclination to the Earth’s equator and the Keplerian mean motion $n = \sqrt{GM/a^3}$, respectively.

Satellite	a (km)	e	i (deg)	n (10^{-4} s^{-1})	$\dot{\Omega}_{\text{LT}}$ (mas yr $^{-1}$)	S/M (m 2 kg $^{-1}$)
LAGEOS	12270	0.0045	109.84	4.643	30.7	6.9×10^{-4}
LAGEOS II	12163	0.0135	52.64	4.710	31.4	7.0×10^{-4}
Ajisai	7870	0.001	50.0	9.042	116.2	5.3×10^{-3}
Jason–1	7713	0.0001	66.04	9.320	123.4	2.7×10^{-2}

4.1 A possible combination of nodes and the gravitational errors

The following combination

$$\delta\dot{\Omega}^{\text{LAGEOS}} + k_1\delta\dot{\Omega}^{\text{LAGEOS II}} + k_2\delta\dot{\Omega}^{\text{Ajisai}} + k_3\delta\dot{\Omega}^{\text{Jason-1}} = \mu_{\text{LT}}49.5, \quad (8)$$

with

$$k_1 = 0.347, \quad k_2 = -0.005, \quad k_3 = 0.068, \quad (9)$$

suitable satellite. However, TOPEX/Poseidon also has a more irregular attitude and solar array behavior, a more complex shape and less precise tracking instrumentation. Its RMS radial orbit accuracy is estimated at 2.8 cm [33].

could be used in order to cancel the effect of the first three even zonal harmonics J_2 , J_4 and J_6 along with their temporal seasonal, stochastic and secular variations. Recently, an analogous approach has been followed [32] by including also some GPS satellites. According to EIGEN-CG01C, the systematic error induced by the remaining uncanceled even zonal harmonics of geopotential amounts to 0.7% only (RSS calculation at $1-\sigma$ level), with an upper bound of 1.6% (sum of the absolute values of the individual errors at $1-\sigma$ level). It must be noted that, contrary to the combination which can be obtained with the nodes of Stella and Starlette instead of that of Jason-1, a calculation up to degree $\ell = 20$ is quite adequate to assess the error due to geopotential. It is so thanks to the higher altitude of Jason-1 with respect to Stella ($a_{\text{Stl}} = 7193$ km) and Starlette ($a_{\text{Str}} = 7331$ km). Contrary to the other examined combinations, in particular the LAGEOS-LAGEOS II two-nodes J_2 -free formula of [20], the secular variations of the even zonal harmonics \dot{J}_ℓ do not affect (8). The combination (8) would not be affected by harmonic perturbations of tidal origin with large amplitudes and particularly long periods. Indeed, the tidal perturbation induced by the tesseral ($m = 1$) K_1 tide, which is one of the most powerful tidal constituents in affecting the orbits of Earth satellites [26], has its period equal to that of the satellite's node; it amounts to -0.47, -0.32, -1.55 and 2.84 years for Jason-1, Ajisai, LAGEOS II and LAGEOS, respectively. This means that a relatively short observational time span could be adopted in order to have it longer than the periods of the most effective perturbations which could then be fitted and removed from the time series [34, 35].

4.2 The impact of the observational errors of Ajisai and Jason-1

In regard to the impact of the measurement errors, let us assume, in a very pessimistic way, that the RMS of the recovered orbits of Ajisai and Jason-1, obtained in a truly dynamical way without resorting to too many empirical accelerations which could absorb also the Lense-Thirring effect, amount to 1 m over, say, 1 year. Then, the error in the nodal rates can be quantified as 26.2 mas and 26.7 mas for Ajisai and Jason-1, respectively. Thanks to the coefficients (9), their impact on the combination (8) would amount to 1.6 mas, i.e. 3.4% of the Lense-Thirring effect over 1 year.

4.3 The impact of the non-gravitational perturbations of Ajisai

Ajisai is a spherical geodetic satellite launched in 1986. It is a hollow sphere covered with 1436 corner cube reflectors (CCR's) for SLR and 318 mirrors to reflect sunlight. Its diameter is 2.15 m, contrary to LAGEOS which has a diameter of 60 cm only. Its mass is 685 kg, while LAGEOS mass is 406 kg. Then, the Ajisai's area-to-mass ratio S/M , which the non-conservative effects are proportional to, is larger than that of the LAGEOS satellites by almost one order of magnitude resulting in a higher sensitivity to surface forces. However, we will show that their impact on the proposed combination (8) should be less than 1%.

4.3.1 The atmospheric drag

The most important non-conservative force in affecting the orbits of the low satellites is the atmospheric drag. Its acceleration can be written as

$$\mathbf{a}_D = -\frac{1}{2}C_D \left(\frac{S}{M} \right) \rho V \mathbf{V}, \quad (10)$$

where C_D is a dimensionless drag coefficient close to 2, ρ is the atmospheric density and \mathbf{V} is the velocity of the satellite relative to the atmosphere (called ambient velocity). Let us write $\mathbf{V} = \mathbf{v} - \boldsymbol{\omega} \times \mathbf{r}$ where \mathbf{v} is the satellite's velocity in an inertial frame. If the atmosphere corotates with the Earth $\boldsymbol{\sigma}$ is the Earth's angular velocity vector $\boldsymbol{\omega}_\oplus = \omega_\oplus \mathbf{k}$, where \mathbf{k} is a unit vector. However, it must be considered that there is a 20% uncertainty in the corotation of the Earth's atmosphere at the Ajisai's altitude⁹. We will then assume $\boldsymbol{\sigma} = \omega_\oplus(1 + \xi)\mathbf{k}$, with $\xi = 0.2$ in order to account for this effect.

Regarding the impact of a perturbing acceleration on the orbital motion, the Gaussian perturbative equation for the nodal rate is

$$\frac{d\Omega}{dt} = \frac{1}{na\sqrt{1-e^2}\sin i} A_N \left(\frac{r}{a} \right) \sin u, \quad (11)$$

where $n = \sqrt{GM/a^3}$ is the Keplerian mean motion, A_N is the out-of-plane component of the perturbing acceleration and $u = \omega + f$ is the satellite's argument of latitude.

⁹It is believed that the atmosphere rotates slightly faster than the Earth at some altitudes with a 10-20% uncertainty (Ries 2004, private communication).

The out-of-plane acceleration induced by the atmospheric drag can be written as [36]

$$A_N^{(\text{atm})} = -\frac{1}{2}K_D\sigma\rho v r \sin i \cos u, \quad (12)$$

with

$$K_D = C_D \left(\frac{S}{M} \right) \sqrt{k_R} \quad (13)$$

and

$$k_R = 1 - \frac{2\sigma h \cos i}{v^2} + \left(\frac{\sigma r \cos \delta}{v} \right)^2. \quad (14)$$

The quantities h and δ are the orbital angular momentum per unit mass and the satellite's declination, respectively. By inserting (12) in (11) and evaluating it on an unperturbed Keplerian ellipse it can be obtained

$$\frac{d\Omega^{(\text{atm})}}{dt} \propto -\frac{1}{2}K_D\rho(1-e^2)\sigma a. \quad (15)$$

It must be pointed out that the density of the atmosphere ρ has many irregular and complex variations both in position and time. It is largely affected by solar activity and by the heating or cooling of the atmosphere. Moreover, it is not actually spherically symmetric but tends to be oblate. A very cumbersome analytic expansion of ρ based on the TD88 model can be found in [36]. In order to get an order of magnitude estimate we will consider a typical value $\rho = 1 \times 10^{-18} \text{ g cm}^{-3}$ at Ajisai altitude [37]. By assuming $C_D = 2.5$ (15) yields a nominal amplitude of 25 mas yr^{-1} for the atmosphere corotation case and 5 mas yr^{-1} for the 20% departure from exact corotation. The impact of such an effect on (8) would be 3×10^{-3} .

4.3.2 The thermal and radiative forces

The action of the thermal forces due to the interaction of solar and terrestrial electromagnetic radiation with the complex physical structure of Ajisai has been investigated in [37]. The temperature asymmetry on Ajisai caused by the infrared radiation of the Earth produces a force along the satellite spin axis direction called Yarkovsky-Rubincam effect. This thermal thrust produces secular perturbations in the orbital elements, but no long-periodic perturbations exist if the spin axis of Ajisai is aligned with the Earth's rotation axis. In fact, the spin axis was set parallel to the Earth rotation axis at orbit insertion. The analogous solar heating (Yarkovsky-Schach effect) is smaller than the terrestrial heating. A nominal secular nodal rate of 15

mas yr⁻¹ due to the Earth heating has been found. It would affect (8) at a 1.5×10^{-3} level.

The effect of the direct solar radiation pressure on Ajisai has been studied in [38]. For an axially symmetric, but not spherically symmetric, satellite like Ajisai there is a component of the radiation pressure acceleration directed along the sun-satellite direction $a_{\odot}^{(\text{iso})}$ and another smaller component perpendicular to the sun-satellite direction. By assuming for the isotropic reflectivity coefficient its maximum value $C_R = 1.035$ the radiation pressure acceleration $a_{\odot}^{(\text{iso})}$ experienced by Ajisai amounts to 2.5×10^{-8} m s⁻². Its nominal impact on the node, proportional to $ea_{\odot}^{(\text{iso})}/4na$, can be quantified as 5.7 mas yr⁻¹; it yields a 5.7×10^{-4} relative error on (8). The anisotropic component of the acceleration would amount, at most, to 2% of the isotropic one, so that its impact on (8) would be totally negligible.

4.4 The impact of the non-gravitational perturbations on Jason-1

The complex shape, varying attitude modes and the relatively high area-to-mass ratio of the satellite (see Table 1), suggest a more complex modelling and higher sensitivity to the non-gravitational accelerations than in the case of the spherical geodetic satellites. On the other hand, important limiting factors in the non-gravitational force modelling of the spherical satellites are attitude and temperature knowledge [21]. These parameters are actually very well-defined and accurately measured [39] on satellites such as Jason-1. A lot of effort has already been put into the modelling of non-gravitational accelerations for TOPEX/Poseidon [40, 41, 42], so that similar models [43] have been routinely implemented for Jason-1. These so-called box-wing models, in which the satellite is represented by eight flat panels, were developed for adequate accuracy while requiring minimal computational resources. A recent development is the work on much more detailed models of satellite geometry, surface properties, eclipse conditions and the Earth's radiation pressure environment for use in orbit processing software [44, ?]. It should be noted that such detailed models were not yet adopted in the orbit analyses of [31]. In fact, their results were based on the estimation of many empirical 1-cycle-per-revolution (cpr) along-track and cross-track acceleration parameters, which absorb all the mismodelled/unmodelled physical effects, of gravitational and non-gravitational origin, which induce secular and long-period changes in the orbital elements. Due to the power of this reduced-dynamic technique, based on the dense tracking data, further im-

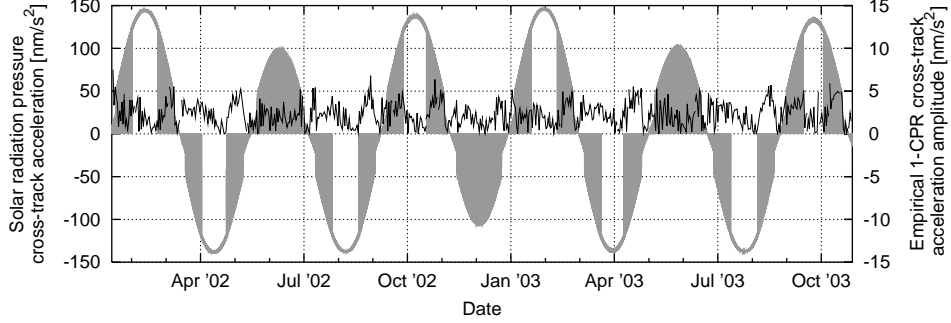


Figure 2: Time series of the modelled Jason-1 out-of-plane solar radiation pressure acceleration (grey) and the estimated 1-cpr out-of-plane acceleration (black, right-hand scale).

provements in the force models become largely irrelevant for the accuracy of the final orbit. Such improved models remain, however, of the highest importance for the determination of $\delta\dot{\Omega}^{\text{Jason-1}}$.

From (11) it can be noted that, since we are interested in the effects averaged over one orbital revolution, the impact of every acceleration constant over such a timescale would be averaged out. The major problems come from 1-cpr out-of-plane accelerations of the form $A_N = S_N \sin u + C_N \cos u$, with S_N and C_N constant over one orbital revolution.

We have analyzed both the output of the non-gravitational force models described in [43] and the resulting residual empirical 1-cpr accelerations estimated from DORIS and SLR tracking over 24-hour intervals. Solar radiation pressure, plotted in figure 2, is by far the largest out-of-plane non-gravitational acceleration, with a maximum amplitude of 147 nm s^{-2} . It is followed by Earth radiation pressure at approximately 7 nm s^{-2} . The contributions of aerodynamic drag and the thermal imbalance force on the cross-track component are both estimated to have a maximum of approximately 0.5 nm s^{-2} . As can be seen in figure 2, the cross-track solar radiation pressure acceleration shows a sinusoidal long-term behavior, crossing zero when the Sun-satellite vector is in the orbital plane, roughly every 60 days. It is modulated by the long-term seasonal variations in Sun-Earth geometry, as well as by eclipses and the changing satellite frontal area, both of which are contributing 1-cpr variations. In fact, the shading of certain areas in figure 2 is due to the effect of the eclipses, which, at once-per-orbit, occur much more frequently than can be resolved in this figure.

As mentioned before, the empirical 1-cpr accelerations absorb the errors

of almost all the unmodelled or mismodelled forces. Now note the systematic way in figure 2, in which the empirical 1-cpr cross-track acceleration drops to values of below 1 nm s^{-2} near the end of each eclipse-free period, and has its maximum level of 5–6 nm s^{-2} only during periods containing eclipses. The fact that the amplitude, but also the phasing (not shown in the figure) of the 1-cpr accelerations show a correlation with the orientation of the orbital plane with respect to the Sun, indicates that it is for a large part absorbing mismodelled radiation pressure accelerations.

By averaging (11) over one orbital revolution and from the orbital parameters of Table 1 it turns out that a 1-cpr cross-track acceleration would induce a secular rate on the node of Jason proportional to $7.6 \times 10^{-5} \text{ s m}^{-1} \times S_N \text{ m s}^{-2}$. This figure must be multiplied by the combination coefficient k_3 . By using the average value of the empirical 1-cpr acceleration from the above analysis $S_N \approx 2.3 \text{ nm s}^{-2}$ as an estimate for the mismodelled non-gravitational forces, it can be argued that the impact on $k_3 \delta \dot{\Omega}^{\text{Jason-1}}$ would amount to 77.4 mas yr^{-1} . However, it must be pointed out that our assumed value of S_N can be improved by adopting the aforementioned more detailed force models or by tuning the radiation pressure models using tracking data. In addition, it must be pointed out that S_N experiences long-term variations mainly induced by the orientation of the orbital plane with respect to the Sun, and the related variations in satellite attitude. For Jason-1 such a periodicity amounts to approximately 120 days (the β' cycle). Let us, now, evaluate what would be the impact of such a long-periodic perturbation on our proposed measurement of the Lense-Thirring effect. Let us write, e.g., a sinusoidal law for the long-periodic component of the weighted nodal rate of Jason-1

$$k_3 \frac{d\Omega}{dt} = (77.4 \text{ mas yr}^{-1}) \times \cos \left[2\pi \left(\frac{t}{P_{\beta'}} \right) \right]; \quad (16)$$

then, if we integrate (16) over a certain time span T_{obs} we get

$$k_3 \Delta\Omega = \left(\frac{P_{\beta'}}{2\pi} \right) (77.4 \text{ mas yr}^{-1}) \times \sin \left[2\pi \left(\frac{T_{\text{obs}}}{P_{\beta'}} \right) \right]. \quad (17)$$

Then, the amplitude of the shift due to the weighted node of Jason-1, by assuming $P_{\beta'} \cong 120$ days, would amount to

$$k_3 \Delta\Omega \leq 4 \text{ mas}. \quad (18)$$

The maximum value would be obtained for

$$\frac{T_{\text{obs}}}{P_{\beta'}} = \frac{j}{4}, \quad j = 1, 3, 5, \dots \cong 30, 90, 150, \dots \text{ days}. \quad (19)$$

So, the impact on the proposed measurement of the Lense–Thirring effect would amount to

$$\left. \frac{\delta\mu_{\text{LT}}}{\mu_{\text{LT}}} \right|_{\text{SRP}} \leq \frac{(4 \text{ mas})}{(49.5 \text{ mas yr}^{-1}) \times (T_{\text{obs}} \text{ yr})}; \quad (20)$$

for, say, $T_{\text{obs}} = 2$ years (20) yields an upper bound of 4%. Moreover, it must also be noted that it would be possible to fit and remove such long–periodic signals from the time series provided that an observational time span longer than the period of the perturbation is adopted, as done in [11].

5 Conclusions

According to the EIGEN-CG01C Earth gravity model, which combines data from CHAMP, GRACE and surface gravimetry/altimetry, the systematic error in the measurement of the Lense–Thirring secular effect due to the mismodelling in the static part of the geopotential is close to a few percent level, at $1\text{-}\sigma$ level, if the combinations (8) is to be used. From this point of view, (8), which is affected by $J_8, J_{10}\dots$ at 1.6% level ($1\text{-}\sigma$), is, at present, better than (5) which, instead, is affected by J_4, J_6, J_8, \dots at a 6% level ($1\text{-}\sigma$). Another advantage of (8) with respect to (5) is that the combination involving Jason-1 and Ajisai is insensitive to the secular variations of the even zonal harmonics, contrary to the two-nodes LAGEOS-LAGEOS II combination which is, instead, affected by the mismodelling in \dot{J}_4 and \dot{J}_6 . This could represent a drawback because their effect grows linearly in time and, at present, the knowledge of \dot{J}_ℓ is rather poor. Their estimated impact on (5) amounts to 1%, at $1\text{-}\sigma$ level, over one year; time spans of more than just one year are required in this kind of analyses.

The price to be paid for the benefits in the reduction of the systematic error of gravitational origin is mainly represented by the non–gravitational perturbations introduced along with the new orbital elements. However, while the bias due to the geopotential is unavoidable because it is constant or grows linearly in time, the signature of the non–conservative accelerations is long-periodic, so that they could be fitted and removed from the time series. This perspective should strongly encourage to explore the possibility of a reanalysis of the Jason–1 orbital data in order to make them suitable to be combined with those from the spherical geodetic satellites. Particular attention should be paid to an as accurate as possible truly dynamical modelling of the non–gravitational accelerations acting on the node of Jason–1. This would be helpful also in other scientific branches related to the Jason-1

activity. It must be noted the non-gravitational perturbations, which are almost negligible on the nodes of the LAGEOS satellites, could represent a major obstacle in using Jason-1. A reasonable estimate of the impact of the non-gravitational perturbations modelling error on Jason-1 on the combination (8) yields an error of the order of 4% over an observational time span of 2 years. However, since the main periodicity of the direct solar radiation pressure perturbation seems to amount to approximately 120 days only, over a time span of a few years it should be possible to average it out or, at least, to fit and remove such biasing signature from the time series. Of course, if the combination (8) will be used, a careful choice of the observational time span would be required in order to reduce the uncertainties related to the orbital maneuvers, which, however, are mainly-although not entirely-in plane, and safe-mode events of Jason-1.

Finally, the obtainable accuracy with the node-node-perigee combination (2), whose error due to geopotential will remain smaller than that of (5)-(8), is strongly related to improvements in the evaluation of the non-gravitational part of the error budget and to the use of time spans many years long. However, it neither seems plausible that the error due to the non-conservative forces acting on the perigee of LAGEOS II will fall to the 1% level nor that a reliable and undisputable assessment of it will be easily obtained. Alternative combinations including the orbital data from the other existing SLR geodetic spherical satellites are, at present, not competitive with the combinations (5) and (8); indeed, the systematic error due to the static part of geopotential amounts to 31% at $1-\sigma$ level.

Acknowledgments

L.I. thanks H. Lichtenegger for Figure 1.

References

- [1] Ciufolini, I., and Wheeler, J.A. (1995). *Gravitation and Inertia*, Princeton University Press, New York.
- [2] Stella, L., et al. (2003). Section E Probing the Gravitomagnetic Lense-Thirring effect with Neutron Stars and Black Holes. In: *Non-linear Gravitodynamics. The Lense-Thirring Effect*, R. Ruffini, and C. Sigismondi (Eds.), World Scientific, Singapore, pp. 235–345.

- [3] Nordtvedt, K. (2003). Some considerations on the varieties of frame dragging. In: *Nonlinear Gravitodynamics. The Lense–Thirring Effect*, R. Ruffini, and C. Sigismondi (Eds.), World Scientific, Singapore, pp. 35–45.
- [4] Schiff, L.I. (1960). On Experimental Tests of the General Theory of Relativity, *Am. J. Phys.* **28**, 340–343.
- [5] Everitt, C.W.F. and other members of the Gravity Probe B team (2001). In: *Gyros, Clocks, Interferometers...: Testing Relativistic Gravity in Space, (Lecture Note in Physics 562)*, C. Lämmerzahl, C.W.F. Everitt, and F.W. Hehl (Eds.), Springer, Berlin, pp. 52–82.
- [6] Lense, J., and Thirring, H. (1918). Über den Einfluss der Eigenrotation der Zentralkörper auf die Bewegung der Planeten und Monde nach der Einsteinschen Gravitationstheorie *Phys. Z.* **19** 156–163, translated by Mashhoon, B., Hehl, F. W., and Theiss, D.S. (1984). On the Gravitational Effects of Rotating Masses: The Thirring-Lense Papers, *Gen. Rel. Grav.* **16**, 711–750.
- [7] Ciufolini, I. (1986). Measurement of Lense–Thirring drag on high-altitude laser ranged artificial satellite, *Phys. Rev. Lett.* **56**, 278–281.
- [8] Iorio, L., Lucchesi, D., and Ciufolini, I. (2002). The LARES mission revisited: an alternative scenario, *Class. Quantum Grav.* **19**, 4311–4325.
- [9] Iorio, L., Ciufolini, I., Pavlis, E.C., Schiller, S., Dittus, H., and Lämmerzahl, C. (2004). On the possibility of measuring the Lense–Thirring effect with a LAGEOS-LAGEOS II-OPTIS mission, *Class. Quantum Grav.* **21**, 2139–2151.
- [10] Lämmerzahl, C., Dittus, H., Peters, A., and Schiller, S. (2001). OPTIS—a satellite-based test of Special and General Relativity, *Class. Quantum Grav.* **18**, 2499–2508.
- [11] Ciufolini, I., Pavlis, E. C., Chieppa, F., Fernandes-Vieira, E., and Pérez-Mercader, J. (1998). Test of General Relativity and Measurement of the Lense–Thirring Effect with Two Earth Satellites, *Science* **279**, 2100–2103.

- [12] Ciufolini, I. (2002). Test of general relativity: 1995–2002 measurement of frame-dragging *Proceedings of the Physics in Collision conference*, Stanford, California, June 20–22, 2002, *Preprint* gr-qc/0209109.
- [13] Ciufolini, I. (1996). On a new method to measure the gravitomagnetic field using two orbiting satellites, *Il Nuovo Cimento A* **109**, 1709–1720.
- [14] Will, C. M. (1993). *Theory and Experiment in Gravitational Physics, 2nd edition*, Cambridge University Press, Cambridge, United Kingdom.
- [15] Will, C. M. (2001). <http://www.livingreviews.org/Articles/Volume4/2001-4will>.
- [16] Ries, J. C., Eanes, R. J., Tapley, B. D., and Peterson, G. E. (2002). Prospects for an Improved Lense-Thirring Test with SLR and the GRACE Gravity Mission *Proceedings of the 13th International Laser Ranging Workshop*, Washington DC, October 7–11, 2002 *Preprint* <http://cddisa.gsfc.nasa.gov/lw13/lw-proceedings.html#science>.
- [17] Ries, J. C., Eanes, R.J., and Tapley, B.D. (2003). Lense-Thirring Precession Determination from Laser Ranging to Artificial Satellites. In: *Nonlinear Gravitodynamics. The Lense–Thirring Effect*, R. Ruffini, and C. Sigismondi (Eds.), World Scientific, Singapore, pp. 201–211.
- [18] Lemoine, F. G., Kenyon, S. C., Factor, J. K., Trimmer, R. G., Pavlis, N. K., Chinn, D. S., Cox, C. M., Klosko, S. M., Luthcke, S. B., Torrence, M. H., Wang, Y. M., Williamson, R. G., Pavlis, E. C., Rapp, R. H., and Olson, T. R. (1998). The Development of the Joint NASA GSFC and the National Imagery Mapping Agency (NIMA) Geopotential Model EGM96 NASA/TP-1998-206861.
- [19] Iorio, L. (2003). The impact of the static part of the Earth’s gravity field on some tests of General Relativity with Satellite Laser Ranging, *Celest. Mech. & Dyn. Astron.* **86**, 277–294.
- [20] Iorio, L. and Morea, A. (2004). The impact of the new Earth gravity models on the measurement of the Lense–Thirring effect, *Gen. Rel. Grav.* **36**, 1321–1333.

- [21] Lucchesi, D. (2001). Reassessment of the error modelling of non-gravitational perturbations on LAGEOS II and their impact in the Lense-Thirring determination. Part I, *Planet. Space Sci.* **49**, 447–463.
- [22] Lucchesi, D. (2002). Reassessment of the error modelling of non-gravitational perturbations on LAGEOS II and their impact in the Lense-Thirring determination. Part II *Planet. Space Sci.* **50**, 1067–1100.
- [23] Pavlis, E. C. (2000). Geodetic Contributions to Gravitational Experiments in Space. In: *Recent Developments in General Relativity*, R. Cianci, R. Collina, M. Francaviglia, and P. Fré (Eds.), Springer-Verlag, Milan, pp. 217–233.
- [24] Iorio, L. (2002). Is it possible to improve the present LAGEOS–LAGEOS II Lense–Thirring experiment?, *Class. and Quantum Grav.* **19**, 5473–5480.
- [25] Reigber, Ch., Schwintzer, P., Stubenvoll, R., Schmidt, R., Flechtner, F., Meyer, U., Knig, R., Neumayer, H., Frste, Ch., Barthelmes, F., Zhu, S.Y., Balmino, G., Biancale, R., Lemoine, J.-M., Meixner, H., and Raimondo, J.C. (2004a). A High Resolution Global Gravity Field Model Combining CHAMP and GRACE Satellite Mission and Surface Gravity Data: EIGEN-CG01C, submitted to *J. of Geod.*
- [26] Iorio, L. (2001). Earth tides and Lense-Thirring effect, *Celest. Mech. & Dyn. Astron.* **79**, 201–230.
- [27] Cox, C., Au, A., Boy, J.-P., and Chao, B. (2002). Time Variable Gravity: Using Satellite Laser Ranging as a Tool for Observing Long-Term Changes in the Earth System *Proceedings of the 13th International Laser Ranging Workshop*, Washington DC, October 7–11, 2002 *Preprint* http://cddisa.gsfc.nasa.gov/lw13/lw_proceedings.html#science.
- [28] Ciufolini, I., and Pavlis, E.C. (2004). A confirmation of the general relativistic prediction of the Lense-Thirring effect, *Nature* **431**, 958–960.
- [29] Reigber, Ch., Schmidt, R., Flechtner, F., König, R., Meyer, U., Neumayer, K.-H., Schwintzer, P., and Zhu, S. Y. (2004b). An Earth

gravity field model complete to degree and order 150 from GRACE: EIGEN-GRACE02S, *J. of Geodynamics* in press.

- [30] Iorio, L. (2004). Some comments about a recent paper on the measurement of the general relativistic Lense-Thirring effect in the gravitational field of the Earth with the laser-ranged LAGEOS and LAGEOS II satellites, preprint gr-qc/0410110.
- [31] Luthcke, S. B., Zelensky, N. P., Rowlands, D. D., Lemoine, F. G., and Williams, T. A. (2003). The 1-Centimeter orbit: Jason-1 Precision Orbit Determination Using GPS, SLR, DORIS, and Altimeter Data, *Marine Geod.* **26**, 399–421.
- [32] Vespe, F., and Rutigliano, P. (2004). The improvement of the Earth gravity field estimation and its benefits in the atmosphere and fundamental physics, paper presented at *35th COSPAR Scientific Assembly Paris, France, 18 - 25 July 2004*, COSPAR04-A-03614, *Adv. Sp. Res.*, submitted.
- [33] Tapley, B. D., Watkins, M. M., Ries, J. C., Davies, G. W., Eanes, R. J., Poole, S. R., Rim, H. J., Schutz, B. E., Shum, C. K., Nerem, R. S., Lerch, F. J., Marshall, J. A., Klosko, S. M., Pavlis, N. K., and Williamson, R. G. (1996). The Joint Gravity Model 3, *J. of Geophys. Res.* **101**, 28029–28049.
- [34] Iorio, L., and Pavlis, E. C. (2001). Tidal Satellite Perturbations and the Lense-Thirring Effect, *J. of the Geod. Soc. of Japan* **47**, 169–173.
- [35] Pavlis, E. C., and Iorio, L. (2002). The impact of tidal errors on the determination of the Lense-Thirring effect from satellite laser ranging, *Int. J. of Mod. Phys. D* **11**, 599–618.
- [36] Abd El-Salam, F.A., and Sehnal, L. (2004). A second order analytical atmospheric drag theory based on the TD88 thermospheric density model, *Celst. Mech. & Dyn. Astron.* in press.
- [37] Sengoku, A., Cheng, M. K., Schutz, B. E., and Hashimoto, H. (1996). Earth-heating effect on Ajisai, *J. of Geod. Soc. of Japan* **42**, 15–27.
- [38] Sengoku, A., Cheng, M. K., and Schutz, B. E. (1995). Anisotropic reflection effect on satellite Ajisai, *J. of Geod.* **70**, 140–145.

- [39] Marshall, J. A., Zelensky, N. P., Klosko, S. M., Chinn, D. S., Luthcke, S. B., Rachlin, K. E., and Williamson, R. G. (1995). The temporal and spatial characteristics of TOPEX/Poseidon radial orbit error, *J. of Geophys. Res.* **100**, 25331–25352.
- [40] Antreasian, P. G., and Rosborough G. W. (1992). Prediction of radiant energy forces on the TOPEX/Poseidon spacecraft, *J. Spacecraft Rockets* **29**, 81–90.
- [41] Marshall, J. A., and Luthcke, S. B. (1994). Radiative force model performance for TOPEX/Poseidon precision orbit determination, *J. Astronaut. Sci.* **49**, 229–246.
- [42] Kubitschek, D. G., and Born, G. H. (2001). Modelling the anomalous acceleration and radiation pressure forces for the TOPEX/POSEIDON spacecraft, *Phil. Trans. R. Soc. Lond. A* **359**, 2191–2208.
- [43] Berthias, J.-P., Piuzzi, A., and Ferrier, C. (2002). Jason postlaunch satellite characteristics for POD activities http://calval.jason.oceanobs.com/html/calval_plan/pod/modele_jason.html
- [44] Doornbos, E., Scharroo, R., Klinkrad, H., Zandbergen, R., and Fritsche, B. (2002). Improved modelling of surface forces in the orbit determination of ERS and Envisat, *Can. J. Remote Sensing* **28**, 535–543.
- [45] Ziebart, M., Adhya, S., Cross, P., Bar-Sever, Y., and Desai, S. (2003). Pixel array solar and thermal force modelling for Jason: On-orbit test results *paper presented at the 'From TOPEX-POSEIDON to Jason' Science Working Team meeting, Arles, France, November 2003.*